Biological role and clinical value of miR-99a-5p in head and neck squamous cell carcinoma (HNSCC): A bioinformatics-based study

Yu-ting Chen[1], Jian-ni Yao[1], Yu-tao Qin[2], Kai Hu[2], Fang Wu[2] and Ye-ying Fang[2] iD

1 Department of Pathology, First Affiliated Hospital of Guangxi Medical University, Nanning, Guangxi, China
2 Department of Radiation Oncology, Radiation Oncology Clinical Medical Research Center of Guangxi, First Affiliated Hospital of Guangxi Medical University, Nanning, Guangxi, China

MicroRNAs (miRNAs) are confirmed to be tumor promoters or suppressors in multiple squamous cell carcinomas (SCCs). miR-99a-5p has been demonstrated to be downregulated in cancerous tissues, but its functional role in head and neck SCC (HNSCC) and its mechanism of action have not been fully elucidated. Here, we studied the expression of miR-99a-5p in HNSCC and performed a clinical value assessment and then extracted mature expression data from The Cancer Genome Atlas (TCGA) and microarrays from Gene Expression Omnibus (GEO). Furthermore, biological analysis was constructed via online prediction tools. The results revealed that miR-99a-5p expression was markedly lower in HNSCC tissues than in normal tissues, which also showed significance in the prognosis of HNSCC. However, its diagnostic value could not be verified due to the lack of body fluid samples. Additionally, miR-99a-5p was expressed at higher levels in patients with low histological grade neoplasms than those with high histological grade neoplasms. The age of the patient might also be a possible clinical parameter affecting miR-99a-5p expression. Furthermore, miR-99a-5p significantly influenced HNSCC progression by regulating the PI3K-Akt signaling pathway, in which the key target genes were upregulated in 519 HNSCC tissues compared to 44 normal tissues, as determined by the Gene Expression Profiling Interactive Analysis (GEPIA). In conclusion, our study may provide insights into the expression and mechanism of miR-99a-5p in HNSCC. Further studies are required to elucidate the role of miR-99a-5p and its potential clinical applications for HNSCC.

Squamous cell carcinomas (SCCs), also known as epidermoid carcinomas, are cancers that derived from squamous epithelial cells, which occur in the head and neck, thyroid, esophagus, lung, penis, prostate, bladder, vagina, and cervix [1–9]. Of these, head and neck SCC (HNSCC) has attracted the

Abbreviations
BP, biological process; CC, cellular component; DAVID, Database for Annotation, Visualization, and Integrated Discovery; FN, false negative; FP, false positive; GEO, Gene Expression Omnibus; GEPIA, Gene Expression Profiling Interactive Analysis; GO, gene ontology; HNSCC, head and neck squamous cell carcinoma; IGF1R, insulin-like growth factor 1 receptor; KEGG, Kyoto Encyclopedia of Genes and Genomes; LR, likelihood ratio; MF, molecular function; MTOR, mechanistic target of rapamycin; PDGFRB, platelet-derived growth factor receptor, beta polypeptide; PIK3CD, phosphatidylinositol-4,5-bisphosphate 3-kinase catalytic subunit data; PPI, protein–protein interaction; ROC, receiver operating characteristic; SCC, squamous cell carcinoma; TCGA, The Cancer Genome Atlas; TN, true negative; TNM, tumor, node, and metastasis; TP, true positive.

attention of researchers due to its significant etiology including tobacco [10], alcohol [11], and human papilloma virus infection [12] associated with people's lifestyles. HNSCCs, the most frequent head and neck neoplasms, are originating from squamous cells in the nasal and oral cavity, paranasal sinuses, pharynx, larynx, and salivary glands. Men are at a higher risk of HNSCC than women. In particular, cancers of the oral cavity and pharynx were reported to cause 49 670 new cases and 9700 deaths worldwide in 2017 and were the ninth highest cause of new cancer cases in men.

A deeper understanding of HNSCC is accompanied with some remarkable explorations for diagnosis, prognosis, and potential pathogenesis [1,13–17]. Current treatment trends include targeted therapy combined with essential chemotherapy, radiotherapy, or immunotherapy [18–23]. Despite this progress, the increasing morbidity, mortality, and complex pathological changes of HNSCC urgently necessitate more effective means for its diagnosis and treatment, especially targeted treatments based on the further exploration of novel biomarkers.

MicroRNAs (miRNAs) are small noncoding RNAs with 21–25 nucleotides, which have been confirmed to be involved in the initiation and development of multiple SCCs [24–29]. Studies have shown significantly aberrant expression of several miRNAs in HNSCCs [27,30–33], indicating that miRNA expression levels may be valuable for the clinical diagnosis and prognosis of HNSCC. There is a strong need to characterize the clinical application of miRNAs for HNSCC. Among validated miRNAs, miR-99a-5p, the major member of miR-99a family, has been demonstrated to be associated with carcinogenesis and deterioration in several cancers such as breast cancer, endometrial carcinoma, osteosarcoma, bladder cancer, lung adenocarcinoma, and hepatocellular carcinoma [34–39]. Several genes have been found to be regulated by miR-99a-5p, which is also enriched in relevant biological pathways [35,40–45].

In HNSCCs, miR-99a-5p has been reported to be downregulated in cancerous tissues [46,47]. Nevertheless, its functional role and relevant mechanism remain to be fully elucidated. In this study, based on the data acquired from Gene Expression Omnibus (GEO), The Cancer Genome Atlas (TCGA), and relevant literature, and using prediction tools (Fig. 1), we calculated the expression level and clinical value of miR-99a-5p, and performed biological analysis. This study might provide a comprehensive explanation of the clinical value and underlying mechanism of miR-99a-5p in HNSCC, to identify abnormally expressed miRNAs involved in HNSCC.
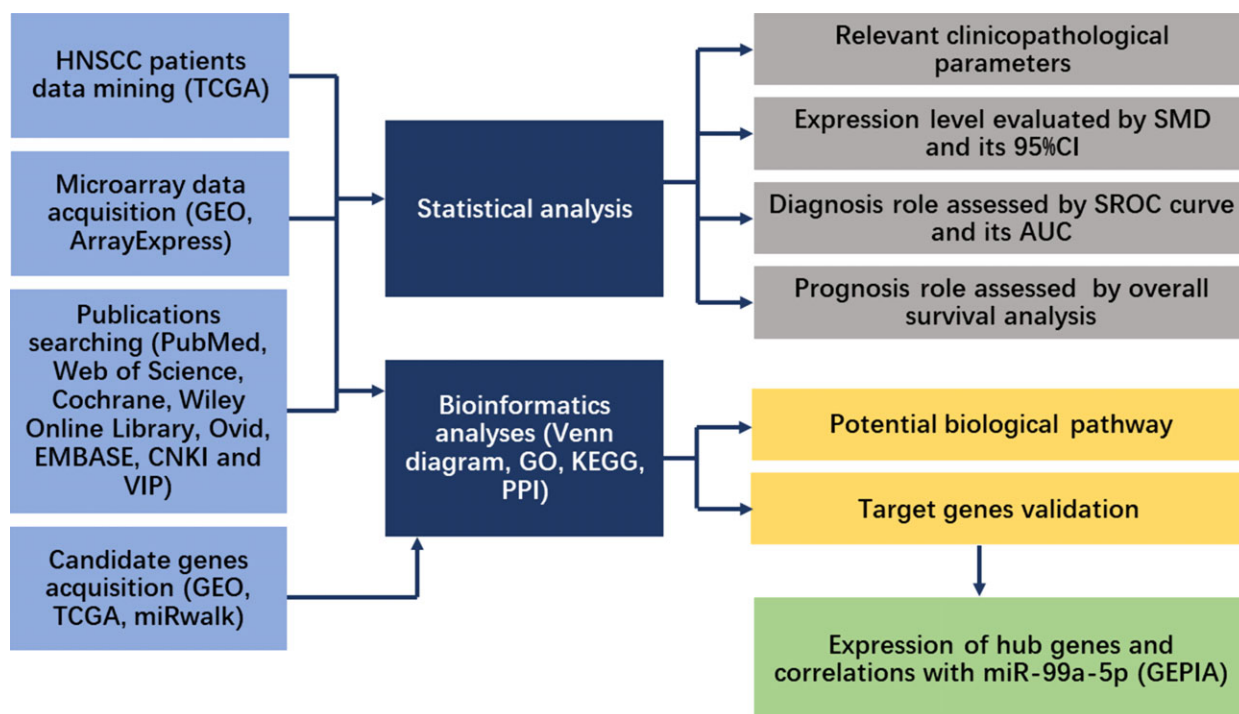
Fig. 1. Flowchart of the study design.

Materials and methods

TCGA data in HNSCC patients

Mature expression data of miR-99a-5p in HNSCC and clinical information were obtained from TCGA datasets via UCSC (http://xena.ucsc.edu/; Accession Number: MIMAT0000097). The IIIuminaHiseq platform included 483 HNSCC patients and 44 adjacent noncancerous head and neck tissues, while the IIIuminaGA platform included 36 patients with HNSCC. No further transformation was performed for the expression data. We explored the possible association between miR-99a-5p expression and clinical parameters for HNSCC patients using the two platforms together or the IIIuminaHiseq platform alone, for further comparison of these two approaches. Based on TCGA data, the diagnostic and prognostic significance of miR-99a-5p was evaluated using the receiver operating characteristic (ROC) curve and the Kaplan–Meier curve, respectively.

Microarray data acquisition and extraction

We obtained available miRNA expression profiling of HNSCC from the GEO database (www.ncbi.nlm.nih.gov/geo/) and ArrayExpress (https://www.ebi.ac.uk/arrayexpress/). The search terms were as follows: ('head AND neck' OR 'laryngeal' OR 'salivary gland' OR 'lip' OR 'mouth' OR 'tongue' OR 'nasopharyngeal' OR 'pharyngeal' OR 'OSCC' OR 'oral squamous cell' OR 'laryngeal' OR 'HNSCC') AND ('carcinoma' OR 'tumor' OR 'cancer' OR 'neoplas*'

OR 'malignan*'). Microarray datasets were eligible with the entry criteria listed below: (1) Patients in each dataset were diagnosed with HNSCC; (2) both cancerous and noncancerous specimens were included in each dataset with a sample size of no less than three per group; and (3) miR-99a-5p expression data should be provided. Several relevant elements were extracted from the microarray datasets: author, publication year, country, platform, sample size, and miR-99a-5p expression level. Two authors (Yu-ting Chen and Jianni Yao) independently extracted essential information from all selected chips. Conflicting opinions were solved by a discussion.

In addition, we searched the PubMed, Web of Science, Cochrane, Wiley Online Library, Ovid, EMBASE, CNKI, and VIP databases for relevant articles. The following strategy was constructed for searching: (microRNA-99 OR hsa-mir-99 OR miR-99 OR MIRN99a microRNA OR microRNA-99a OR miR-99a OR hsa-mir-99a OR MIRN99A OR mir-99a) AND ('head AND neck' OR 'laryngeal' OR 'salivary gland' OR 'lip' OR 'mouth' OR 'tongue' OR 'nasopharyngeal' OR 'pharyngeal' OR 'OSCC' OR 'oral squamous cell' OR 'laryngeal' OR 'HNSCC') AND ('carcinoma' OR 'tumor' OR 'cancer' OR 'neoplas*' OR 'malignan*'). Studies that provided case numbers, mean, and standard deviation (SD) were included.

Statistical analysis

Statistical analyses were performed using SPSS 23.0 (IBM, NY, USA) and Stata version 12.0. Scatter diagrams were

Table 1. Relationships between the expression value of miR-99a-5p and clinicopathological parameters in HNSCC patients based on the IIIuminaHiseq platform.

Clinicopathological features		n	miR-99a-5p expression level	P value
Tissue	Noncancerous	44	10.348 ± 0.625	< 0.001
	Cancerous	483	7.987 ± 1.467	
Gender	Male	351	8.046 ± 1.515	0.152
	Female	132	7.831 ± 1.323	
Age	≥ 50	405	8.040 ± 1.424	0.061
	< 50	77	7.698 ± 1.660	
T	T1–T2	172	8.092 ± 1.477	0.05
	T3–T4	251	7.817 ± 1.371	
N	N0	163	8.005 ± 1.374	0.308
	N1–N3	227	7.854 ± 1.482	
M	M0	174	8.008 ± 1.482	0.139
	M1	1		
Stage	I–II	109	8.140 ± 1.239	0.282
	III–IV	361	7.968 ± 1.525	
Histologic grade	G1–G2	341	7.816 ± 1.393	0.001
	G3–G4	122	8.332 ± 1.582	
Lymphovascular invasion	Yes	113	7.968 ± 1.458	0.180
	No	211	7.747 ± 1.388	
Alcohol	Yes	319	8.046 ± 1.445	0.194
	No	156	7.859 ± 1.521	

Table 2. Relationships between the expression value of miR-99a-5p and clinicopathological parameters in HNSCC patients based on the IIluminaHiseq and IIluminaGA platforms.

| Clinicopathological features		*n*	miR-99a-5p expression level	*P* value
Tissue	Noncancerous	44	10.348 ± 0.625	0.001
	Cancerous	519	8.028 ± 1.498	
Gender	Male	379	8.079 ± 1.558	0.198
	Female	140	7.889 ± 1.317	
Age	≥ 50	436	8.090 ± 1.453	0.027
	< 50	82	7.691 ± 1.695	
T	T1 ~ T2	184	8.097 ± 1.475	0.117
	T3 ~ T4	272	7.882 ± 1.402	
N	N0	175	8.034 ± 1.386	0.314
	N1 ~ N3	245	7.890 ± 1.486	
M	M0	187	8.076 ± 1.488	0.153
	M1	1		
Stage	I–II	115	8.174 ± 1.267	0.300
	III–IV	390	8.010 ± 1.559	
Histologic grade	G1–G2	368	7.841 ± 1.410	0.001
	G3–G4	130	8.413 ± 1.622	
Lymphovascular invasion	Yes	122	7.988 ± 1.451	0.282
	No	229	7.814 ± 1.424	
Alcohol	Yes	346	8.065 ± 1.474	0.366
	No	164	7.936 ± 1.563	

plotted for each study using GraphPad Prism 7.0. We also used SPSS 23.0 to calculate the mean ± SD for all the studies based on the expression value of miR-99a-5p. Stata version 12.0 was used to perform continuous variable meta-analysis by evaluating the overall SMD and 95% CI. Both fixed-effect and random-effect model were employed, while the heterogeneity was analyzed by chi-square and I^2 tests. Sensitivity analysis was added to explain the heterogeneity. Results were considered statistically significant if the observed SMD with 95%CI did not cross 0. Additionally, we constructed Begg's funnel and Egger's plot to detect publication bias.

For diagnostic tests, we used SPSS 23.0 to plot the ROC curve and to calculate the true positive (TP), false positive (FP), false negative (FN), and true negative (TN) for each included study. Then, diagnosis meta-analysis was performed via MetaDisc 1.4. Sensitivity, specificity, positive likelihood ratio (+LR), negative likelihood ratio (−LR), and diagnostic odds ratio (OR), as well as the summarized ROC curve (SROC), were chosen to describe the possible diagnostic value of miR-99a-5p for HNSCC. For practical application, we made a conclusion via the overall consideration of our diagnosis test results and the provided body fluid samples.

Bioinformatics analyses

To predict the putative target genes of miR-99a-5p, we acquired candidate genes from GSE85614 (log2FC < 0), TCGA database (log2FC > 1 and *P* < 0.05). The miR-walk 2.0, which included miRWalk, Targetscan, miR-anda, miRDB, miRNAMap, miRBridge, RNA22, miRMap, PITA, RNAhybrid, PicTar, and Microt4, was
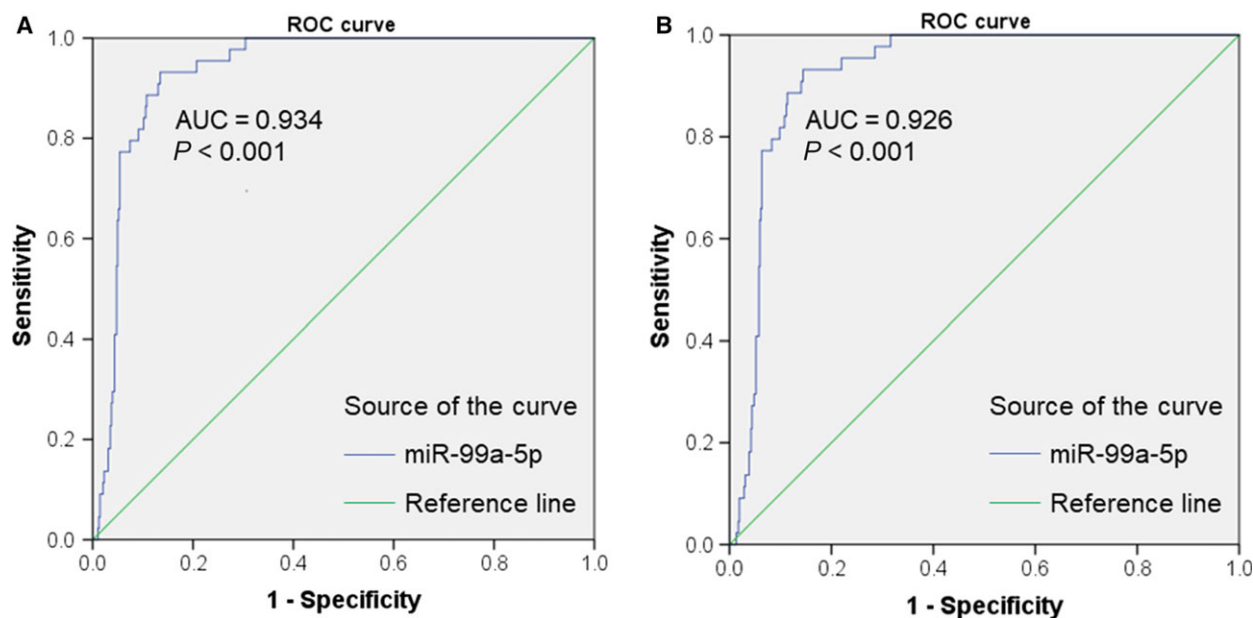
Fig. 2. Receiver operating characteristic (ROC) curves of miR-99a-5p in HNSCC based on TCGA data. (A) Diagnostic value of miR-99a-5p for HNSCC based on the IIluminaHiseq platform (AUC = 0.934, *P* < 0.001). (B) Diagnostic value of miR-99a-5p for HNSCC based on the IIluminaHiseq and IIluminaGA platforms (AUC = 0.926, *P* < 0.001).
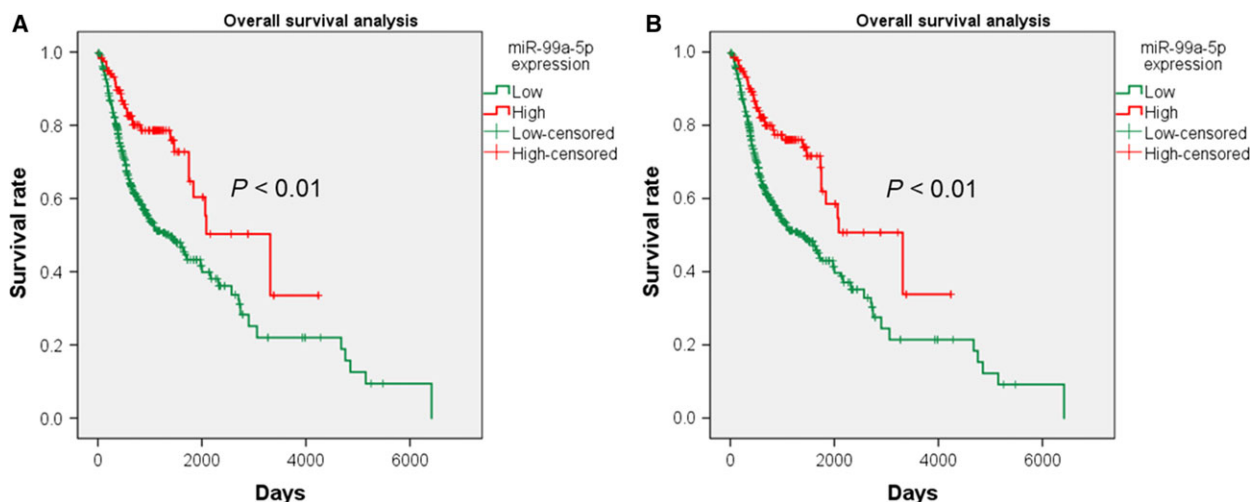
Fig. 3. Kaplan–Meier curves of different miR-99a-5p expression levels based on TCGA data. (A) The overall survival of HNSCC patients varies with different miR-99a-5p expression levels based on the IlluminaHiseq platform ($P < 0.01$). (B) The overall survival of HNSCC patients varies with different miR-99a-5p expression levels based on the IlluminaHiseq and IlluminaGA platforms ($P < 0.01$).

Table 3. Basic characteristics and data of the included microarrays.

| Accession	Author	Year	Country	Platform	Sample	Exp mean ± Exp SD	Ctrl mean ± Ctrl SD	TP	FP	FN	TN
GSE11163	Avissar M *et al.*	2008	USA	GPL6680	21	8.952 ± 1.693	10.531 ± 0.792	12	1	4	4
GSE22587	Li T *et al.*	2013	China	GPL8933	12	560.969 ± 304.226	540.273 ± 73.556	3	0	5	4
GSE28100	Jung HM *et al.*	2012	USA	GPL10850	20	8.151 ± 1.449	8.167 ± 1.431	15	2	2	1
GSE31277	Severino P *et al.*	2014	Brazil	GPL4133	30	13.218 ± 0.97	14.45 ± 0.418	15	2	0	13
GSE32906	Luo Z *et al.*	2012	China	GPL11350	22	6780.977 ± 3169.49	3233.222 ± 1786.07	16	6	0	0
GSE32960	Ma J *et al.*	2012	China	GPL14722	330	9.913 ± 0.808	11.433 ± 0.888	242	3	70	15
GSE34496	Ochs MF *et al.*	2013	USA	GPL8786	69	7.215 ± 1.202	7.762 ± 0.858	27	8	17	17
GSE36682	Wei R *et al.*	2012	China	GPL15311	68	12.56 ± 1.001	13.513 ± 0.391	40	0	22	6
GSE41268	Xie Z *et al.*	2012	China	GPL10850	10	5.978 ± 0.995	5.499 ± 0.703	1	0	6	3
GSE43039	Li X *et al.*	2015	China	GPL16414	40	−0.053 ± 3.322	−0.515 ± 1.23	2	0	18	20
GSE43329	Zheng X *et al.*	2013	China	GPL16475	50	102.21 ± 30.963	98.606 ± 0.583	6	2	25	17
GSE45238	Shiah S *et al.*	2015	Taiwan	GPL8179	80	4094.715 ± 2167.8	9774.709 ± 1957.02	38	4	2	36
GSE46172	Plieskatt JL *et al.*	2014	USA	GPL16770	8	8.262 ± 2.384	9.443 ± 0.614	2	0	2	4
GSE62819	Lian M *et al.*	2014	China	GPL16384	10	10.288 ± 1.185	11.078 ± 1.012	4	1	1	4
GSE69002	Creighton C *et al.*	2016	USA	GPL18044	7	3.305 ± 0.058	3.405 ± 0.115	3	2	0	2
GSE70970	Bruce J *et al.*	2015	Canada	GPL20699	263	9.078 ± 2.033	9.421 ± 0.891	73	1	173	16
GSE82064	Valeri N *et al.*	2017	Switzerland	GPL21968	96	212.885 ± 194.605	139.667 ± 60.085	21	4	57	14

also applied to selected genes with a computer algorithm. Genes overlapping at least two prediction platforms were selected. Based on the above source, prospective genes were screened through intersection by online tools (http://bioinformatics.psb.ugent.be/webtools/Venn/). Meanwhile, validated genes from publications were also added.

Based on the predicted target genes, we conducted Gene ontology (GO) and Kyoto Encyclopedia of Genes and Genomes (KEGG) pathway analysis using online tools (https://david.ncifcrf.gov/) to determine the underlying mechanism of miR-99a-5p in HNSCC. The STRING database (https://string-db.org/) was also utilized to construct a PPI network for further characterizing the interactions among promising target genes of miR-99a-5p. Furthermore, hub genes with over five degrees were selected. In addition, we acquired differentially expressed
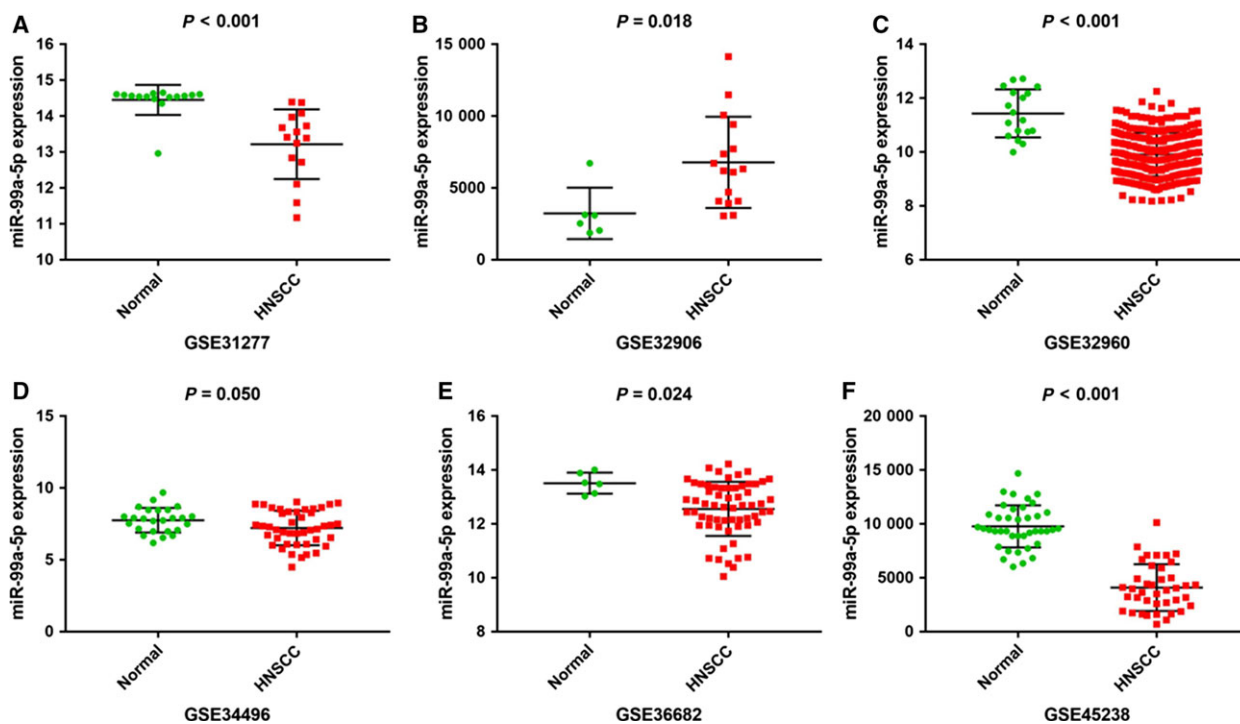
Fig. 4. Representative scatter plots of miR-99a-5p expression data in normal and HNSCC tissues in microarrays. Expression data of miR-99a-5p in normal and HNSCC tissues from microarrays with *P* value ≤ 0.05 were plotted: (A) GSE31277 (*P* < 0.001). (B) GSE32906 (*P* = 0.018). (C) GSE32960 (*P* < 0.001). (D) GSE34496 (*P* = 0.050). (E) GSE36682 (*P* = 0.024). (F) GSE45238 (*P* < 0.001).
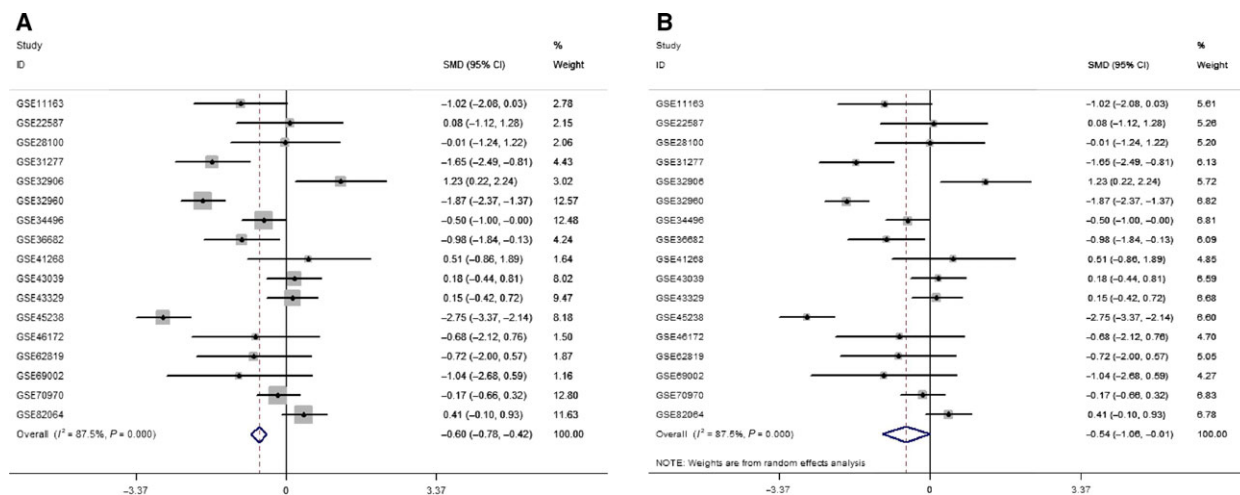
Fig. 5. MiR-99a-5p expression levels in normal tissue and HNSCC by forest plot. (A) Forest plot constructed by the fixed-effect model (SMD = −0.60, 95% CI= −0.78 to −0.42, I^2 = 87.5%). (B) Forest plot constructed by the random-effect model (SMD = −0.54, 95% CI = −1.06 to −0.01, I^2 = 87.5%).

genes of HNSCC from the Gene Expression Profiling Interactive Analysis (GEPIA) (|log2FC| > 1.5, *P* < 0.05) and conducted another KEGG pathway analysis to detect the potential pathways for the progression of HNSCC.

Expression of hub genes and their correlations with miR-99a-5p

Based on GEPIA [48], we detected the expression of hub genes in HNSCC and normal tissues to further identify the

target genes of miR-99a-5p. We also performed Spearman's correlation analysis to explain the correlation between hub genes and miR-99a-5p. Besides, the protein level of those hub genes was acquired from The Human Protein Atlas.

Results

Relationships between miR-99a-5p expression and clinicopathological parameters in HNSCC

Statistical analysis based on the IIIuminaHiseq platform (Table 1) revealed that miR-99a-5p was expressed at a lower level in HNSCC tissues than in normal tissues (7.987 ± 1.467 vs 10.348 ± 0.625, respectively; $P < 0.001$). In addition, miR-99a-5p was expressed at higher levels in G1–G2 than in G3–G4 neoplasms

(8.140 ± 1.239 vs 7.968 ± 1.525, respectively, $P = 0.001$). When statistical analysis was carried out using a combination of the IIIuminaHiseq and IIIuminaGA platforms (Table 2), the results revealed that miR-99a-5p was expressed at lower levels in HNSCC tissues than in adjacent normal tissues (8.028 ± 1.498 vs 10.348 ± 0.625, respectively, $P < 0.001$). Significant differences were also observed among neoplasms of different histological grades (7.841 ± 1.410 vs 8.413 ± 1.622, respectively, $P < 0.001$). In addition, miR-99a-5p expression was higher in patients over 50 years than in those less than 50 years (8.090 ± 1.453 vs 7.691 ± 1.695, respectively, $P = 0.027$). As for the diagnostic test based on TCGA, miR-99a-5p might show significant diagnostic value for HNSCC (AUC = 0.934, $P < 0.001$; AUC = 0.926, $P < 0.001$; Fig. 2). However, the tissue
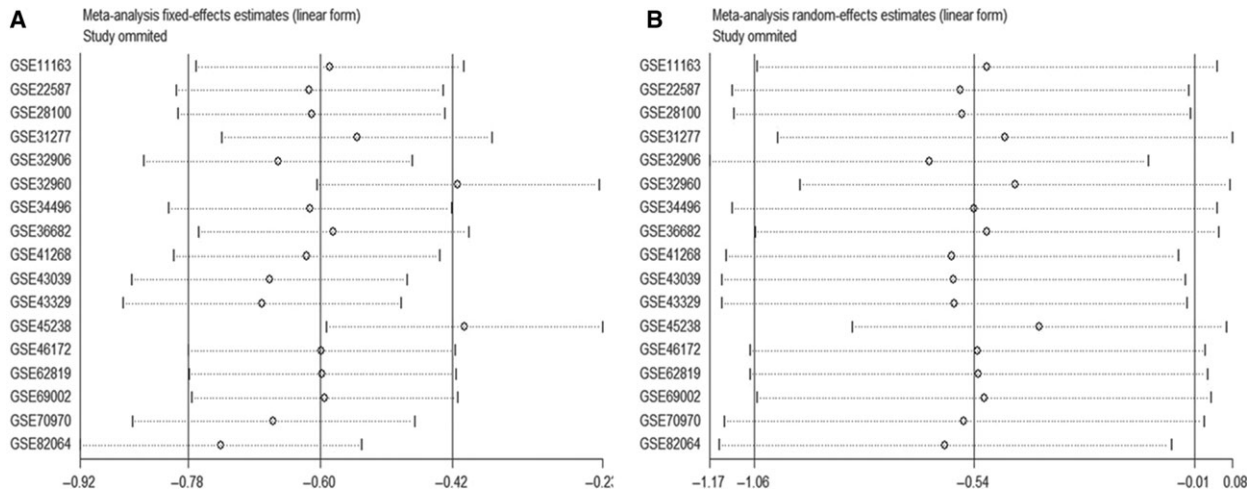
Fig. 6. Sensitivity analysis. (A) Fixed-effect model. (B) Random-effect model. GSE45238 and GSE32960 might be sources of heterogeneity according to the fixed-effect model.
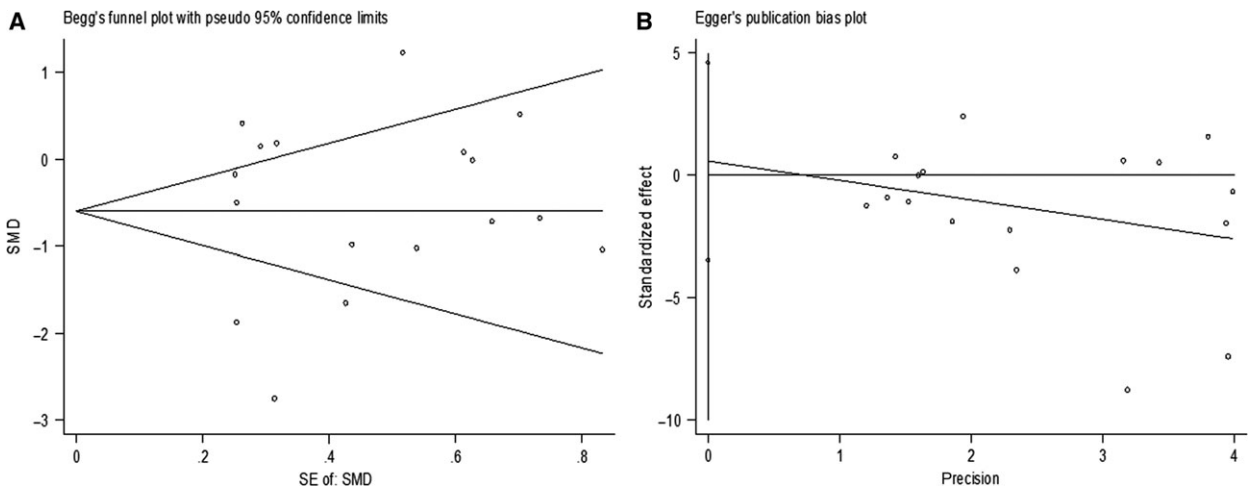

Fig. 7. Publication bias detection. (A) Begg's funnel. (B) Egger's plot.

types of patients were unknown. Additionally, survival analysis indicated a probable prognostic value for HNSCC patients ($P < 0.01$; Fig. 3). The added IIIumi-naGA platform did not significantly affect our research; nevertheless, it reminds us of the need for more samples for further exploration of the relationships between miR-99a-5p expression and clinicopathological parameters of HNSCC patients.

Comprehensive meta-analysis based on microarrays

MiR-99a-5p expression level in HNSCC

A total of 18 eligible microarrays were selected from GEO datasets. Finally, 924 HNSCC tissues and 212 noncancerous head and neck tissues were included as GSE34496 and GSE73460 acted equally. However, no
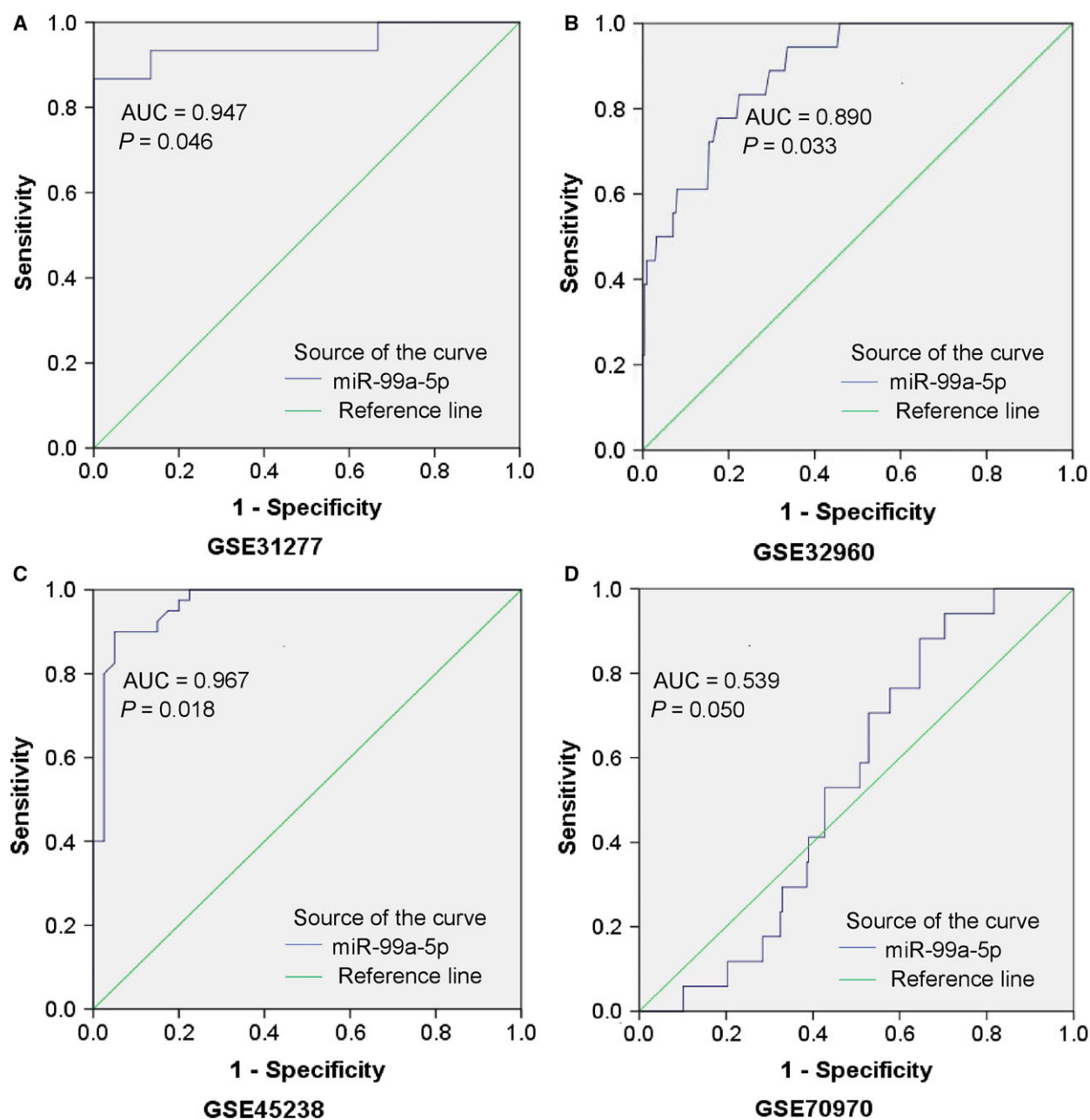
Fig. 8. Representative ROC curves of the microarrays. ROC curve of miR-99a-5p expression in normal and HNSCC tissues from microarrays with *P* value ≤ 0.05 were plotted: (A) GSE31277 (AUC = 0.947, *P* = 0.046). (B) GSE32960 (AUC = 0.890, *P* = 0.033). (C) GSE45238 (AUC = 0.967, *P* = 0.018). (D) GSE70970 (AUC = 0.539, *P* = 0.050).

publications met our criteria. Then, continuous variable meta-analysis pooled the expression data from 17 microarrays (Table 3), among which there were 6 significant microarrays ($P \leq 0.05$; Fig. 4). Other microarrays without statistical significance were displayed in Fig. S1 (A-K). As the overall result revealed, miR-99a-5p expression was lower in HNSCC tissue than in the control group both for fixed-effect (SMD = −0.60, 95% CI = −0.78 to −0.42, I^2 = 87.5%) and random-effect (SMD = −0.54, 95% CI = −1.06 to −0.01, I^2 = 87.5%) models (Fig. 5). Sensitivity analysis was then carried out to evaluate the influence of each chip. GSE45238 and GSE32960 might be the sources of heterogeneity (Fig. 6). Additionally, Begg's funnel and Egger's plot indicated no obvious publication bias (Fig. 7).

Diagnostic value of miR-99a-5p for HNSCC

ROC curves for all eligible studies were plotted. Four representative ROC curves including GSE31277, GSE32960, GSE36682 and GSE45238 were displayed in Fig. 8, with P value less than 0.05, while the other studies showing no statistical significance were in Fig. S1 (L-X). Further analysis was performed based on the TP, FP, FN, and TN results (Table 3). As shown in Fig. 9, the SROC curve verified the diagnostic value of

miR-99a-5p in HNSCC as the AUC was 0.85 (95% CI = 0.77–0.92), with a sensitivity of 0.56 (95%CI=0.52–0.59, $P < 0.001$) and a specificity of 0.85 (95% CI = 0.80–0.90, $P = 0.030$). Furthermore, likelihood ratios were calculated (Pool +LR = 2.90, 95% CI = 1.91–4.39, $P = 0.074$; pool −LR = 0.52, 95% CI = 0.38–0.73, $P < 0.001$), respectively. The diagnostic OR of 8.23 (95% CI = 3.71–18.25, $P = 0.006$) also suggested a significant diagnostic value when based on all the included samples. However, only the GSE41268 and GSE69002 chips provided body fluid samples (AUC = 0.333, $P = 0.201$ and AUC = 0.750, $P = 0.197$, respectively). Thus, the clinical diagnostic value of miR-99a-5p for HNSCC could not be fully verified.

Bioinformatics analyses of miR-99a-5p and HNSCC

Prediction of miR-99a-5p target genes

We screened 14 174 genes from GSM2279805, 1532 genes from the TCGA dataset, and 3085 genes from miRwalk 2.0 after removing duplicates. As the analytical integration shown, a total of 98 genes overlapped in the GSM microarray and online software (Fig. 10). *MTMR3, IGF1R, MTOR, NOX4,* and *HOXA1*, which were searched from published literature, were also
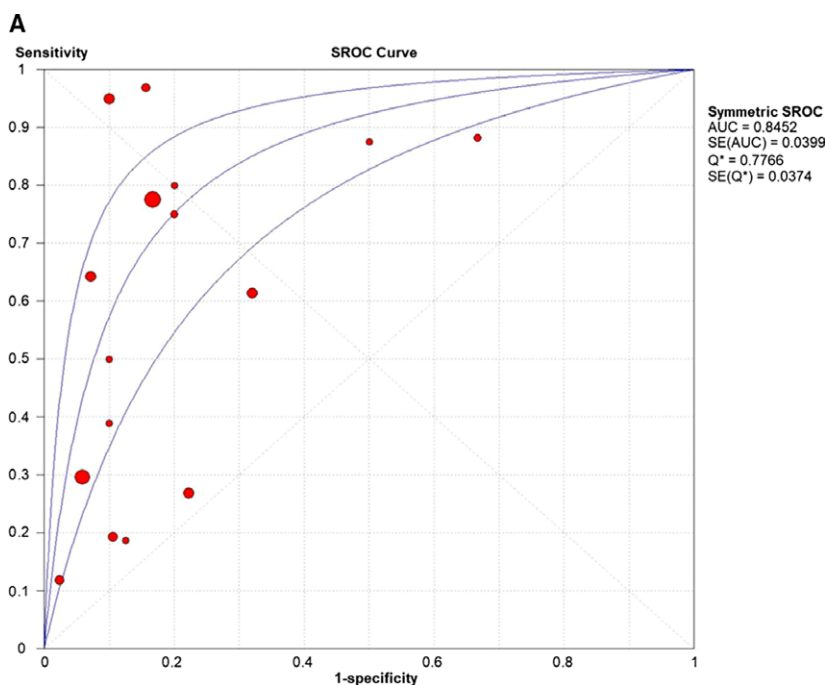
Fig. 9. Diagnostic test based on the 17 included microarrays. (A) The summarized receiver operating characteristic (SROC) curve (AUC = 0.85, 95% CI = 0.77–0.92 calculated manually). (B) Sensitivity value of 0.56 (95%CI = 0.52–0.59, $P < 0.001$). (C) Specificity value of 0.85 (95% CI = 0.80–0.90, $P = 0.030$). (D) Pool positive likelihood ratio of 2.90 (95% CI = 1.91–4.39, $P = 0.074$). (E) Pool negative likelihood ratio of 0.52 (95% CI = 0.38–0.73, $P < 0.001$). (F) Diagnostic odds ratio of 8.23 (95% CI = 3.71–18.25, $P = 0.006$).

included [49–53]. Finally, a total of 103 genes were identified as the promising target genes of miR-99a-5p in HNSCC (Table 4).

GO enrichment and KEGG pathway analysis

For GO enrichment analysis, the results comprised biological process (BP), cellular component (CC), and molecular function (MF). The potential target genes of miR-99a-5p significantly influence 15 GO terms

($P < 0.05$), including cell migration and phosphatidylinositol-mediated signaling in BP, and focal adhesion in CC. Additionally, KEGG pathway analysis also indicated that the PI3K-Akt signaling pathway and pathways in cancer were the most enriched for miR-99a-5p in HNSCC ($P < 0.001$, FDR < 0.05; Fig. 11). According to another KEGG pathway analysis, the PI3K-Akt signaling pathway and pathways in cancer were also confirmed to be significant in the progression of HNSCC ($P < 0.001$; Fig. 12).
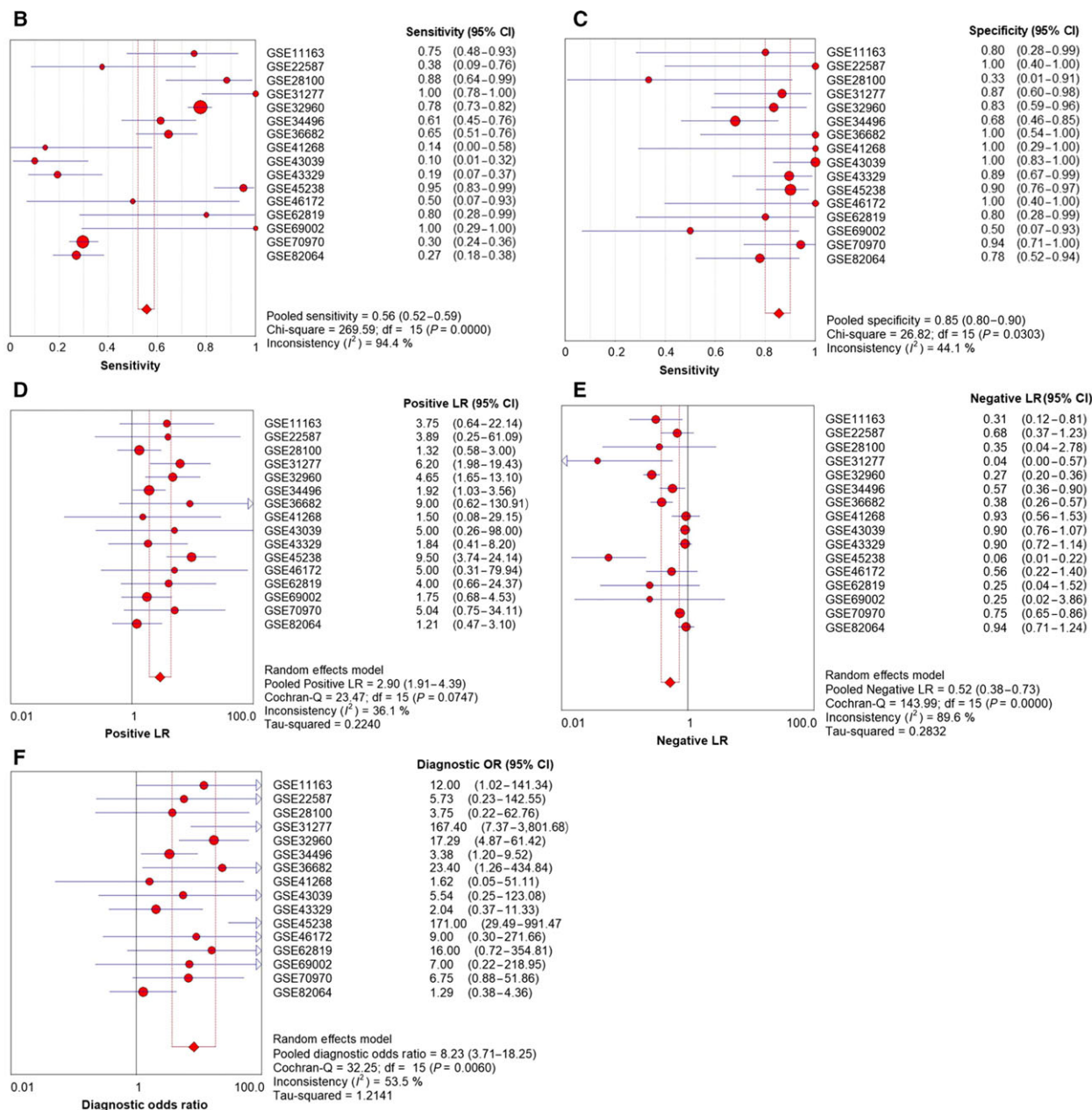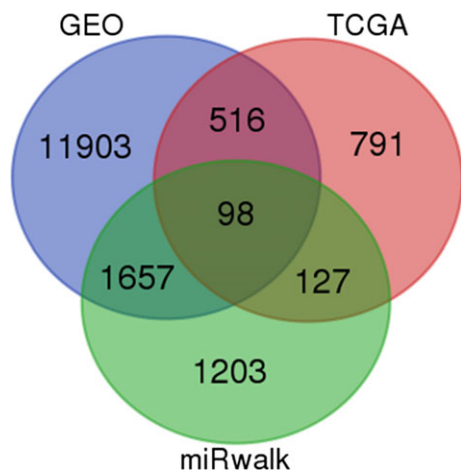

Fig. 9. (Continued)

Fig. 10. Venn diagram for identifying 98 promising target genes of miR-99a-5p in HNSCC.

PPI network construction

The 103 putative target genes were inputted into STRING for constructing a PPI network (Fig. 13). There were 103 nodes and 49 edges with an enrichment *P* value of 0.007. Thus, we further identified *PIK3CD*, *IGF1R*, *PDGFRB*, and *MTOR* as the hub genes of miR-99a-5p in HNSCC (all degrees > 5).

Expression value of hub genes and their correlations with miR-99a-5p

As shown in the boxplot (Fig. 14), *PIK3CD*, *IGF1R*, *PDGFRB*, and *MTOR* all exhibited higher expression

levels in 519 HNSCC tissues compared to the 44 normal tissues. *PIK3D* and *IGFR1* expression levels were significant negatively correlated to miR-99a-5p in HNSCC (PIK3D: $r = -0.318$, $P < 0.001$; IGFR1: $r = -0.118$, $P = 0.005$), while PDGFRB and MTOR were mildly negatively correlated with miR-99a-5p (PDGFRB: $r = -0.036$, $P = 0.393$; MTOR: $r = -0.012$, $P = 0.774$; Fig. 15).

Discussion

There has been a trend of targeted treatment for human cancers in recent years. Illuminated by the abnormal biological signals in cancer cells, people commit to detecting novel biomarkers for exploring the potential mechanism of tumorigenesis and progression as well as further clinical applications such as cancer diagnosis, treatment, and prognosis. Therein, the miRNAs, which appear to be involved in gene regulation, were confirmed to be tumor suppressors or promoters [54,55].

Several studies have demonstrated that miR-99a-5p could affect proliferation, migration, and invasion in various cancers, including HNSCCs, via modulating gene expression [36,56,57]. The reduced miR-99a-5p expression was confirmed to suppress the insulin-like growth factor mammalian of rapamycin signaling (IGF-mTOR signaling) through binding sites in their 3′-untranslated regions (UTRs) in childhood adrenocortical tumors [58]. According to Kuo *et al.*, miR-99a-5p could inhibited myotubularin-related protein 3 (MTMR3) expression then suppress the metastasis of

Table 4. Validated genes of miR-99a-5p from the GEO, TCGA, and miRwalk databases and literature.

	Genes					
Validated in HNSCC	MTMR3	IGF1R	MTOR	NOX4	HOXA1	
Validated by analytical integration	LAMA5	AGO2	HIP1	SLC44A1	TNFAIP8L1	POLE
	RELB	U2SURP	RNF213	DNASE2	MPP3	TRAM2
	LHFPL2	NCS1	FAM64A	TTYH3	HSP90B1	GUCY1A3
	WNT7B	CELSR1	SLC39A14	MXRA8	NRIP3	PAPLN
	ASNS	PIK3CD	NAV1	FANCA	STK10	AFAP1L1
	B4GALNT1	TAPBP	WARS	TUSC3	CASK	PRSS23
	HENMT1	ACVR1	ANGPT2	BICD1	DLX5	RGS3
	ABCG1	ITGA3	SH2B3	COL5A1	CTLA4	ECE1
	ETS1	EXT2	FOXM1	BCAM	MN1	PDGFRB
	PYCR1	MAPK12	SLC1A4	GPR68	STC2	UBE2L6
	SCRN1	IGF2BP2	TSPAN9	SLC2A6	KIAA0930	FLRT2
	TMEM184B	DKK3	EPB41L4B	KIRREL	YEATS2	IPO9
	FAM111A	STRA6	ORAI2	LBH	APH1B	KRBA1
	RNASE7	MARVELD3	C1QTNF1	ANTXR2	GJB4	C10orf35
	NPNT	SH3PXD2B	ADAM8	COL6A2	HAS2	ODC1
	TGFB3	FADD	DDIT4	MISP	MFAP5	SYT7
	ARHGEF39	NRBP2				

Category	Term	Count		%		P value
KEGG_PATHWAY	cfa04151:PI3K-Akt signaling pathway	11		0.06375		0.00003
	cfa05200:Pathways in cancer	10		0.05795		0.00053
	cfa04550:Signaling pathways regulating pluripotency of stem cells	6		0.03477		0.00146
	cfa04510:Focal adhesion	7		0.04057		0.00158
	cfa05215:Prostate cancer	5		0.02898		0.00195
	cfa05166:HTLV-I infection	7		0.04057		0.00376
	cfa05214:Glioma	4		0.02318		0.00739
	cfa04512:ECM-receptor interaction	4		0.02318		0.01633
	cfa05231:Choline metabolism in cancer	4		0.02318		0.02297
	cfa04066:HIF-1 signaling pathway	4		0.02318		0.02483
	cfa05142:Chagas disease (American trypanosomiasis)	4		0.02318		0.02611
	cfa05146:Amoebiasis	4		0.02318		0.02743
	cfa05205:Proteoglycans in cancer	5		0.02898		0.03169
	cfa05145:Toxoplasmosis	4		0.02318		0.03379
	cfa04015:Rap1 signaling pathway	5		0.02898		0.03823
	cfa04611:Platelet activation	4		0.02318		0.04337
	cfa04014:Ras signaling pathway	5		0.02898		0.04487
	cfa04068:FoxO signaling pathway	4		0.02318		0.04683
	cfa04150:mTOR signaling pathway	3		0.01739		0.05132
	cfa05230:Central carbon metabolism in cancer	3		0.01739		0.05607
	cfa05218:Melanoma	3		0.01739		0.07117
	cfa05222:Small cell lung cancer	3		0.01739		0.09501
	cfa04914:Progesterone-mediated oocyte maturation	3		0.01739		0.09886
GOTERM_BP_DIRECT	GO:0030335~positive regulation of cell migration	5		0.02898		0.00777
	GO:0048015~phosphatidylinositol-mediated signaling	3		0.01739		0.00788
	GO:0050890~cognition	3		0.01739		0.01023
	GO:0060325~face morphogenesis	3		0.01739		0.01194
	GO:0032964~collagen biosynthetic process	2		0.01159		0.02540
	GO:0016242~negative regulation of macroautophagy	2		0.01159		0.04404
	GO:0043206~extracellular fibril organization	2		0.01159		0.04404
	GO:0043583~ear development	2		0.01159		0.04404
	GO:0030154~cell differentiation	4		0.02318		0.06085
	GO:0006810~transport	3		0.01739		0.06516
	GO:0001666~response to hypoxia	3		0.01739		0.07231
	GO:0048260~positive regulation of receptor-mediated endocytosis	2		0.01159		0.07432
	GO:0050905~neuromuscular process	2		0.01159		0.08026
	GO:0030325~adrenal gland development	2		0.01159		0.08616
	GO:0060037~pharyngeal system development	2		0.01159		0.09203
	GO:0001764~neuron migration	3		0.01739		0.09318
GOTERM_CC_DIRECT	GO:0005925~focal adhesion	7		0.04057		0.00901
	GO:0005886~plasma membrane	19		0.11011		0.01293
	GO:0048471~perinuclear region of cytoplasm	7		0.04057		0.01427
	GO:0009897~external side of plasma membrane	5		0.02898		0.01624
	GO:0005604~basement membrane	3		0.01739		0.03079
	GO:0070062~extracellular exosome	20		0.11590		0.04631
	GO:0005829~cytosol	11		0.06375		0.04766
	GO:0002102~podosome	2		0.01159		0.06518
	GO:0005794~Golgi apparatus	7		0.04057		0.06798
GOTERM_MF_DIRECT	GO:0005524~ATP binding	12		0.06954		0.06223

Fig. 11. Functional annotation of target genes by GO enrichment and KEGG pathway analysis (P value < 0.05 for KEGG, BP, and CC).

oral cancer (OC) [49]. As for HNSCC, Chen et al. also reported that IGFR1 and MTOR were repressed by ectopic transfection of miR-99-5p [51]. In addition, Yan et al. suggested that downregulation of miR-99a-5p contributed to oral squamous cell carcinoma (OSCC) by targeting MTOR, further indicating the relation between miR-99a-5p and HNSCC

development [59]. Recently, miR-99a-5p was found to facilitate oral tumor cells by targeting NADPH oxidase 4 (NOX4) [52]. To achieve a deeper understanding of the mechanism underlying miR-99a-5p, we identified its potential targets and performed the comprehensive biological pathway analysis. According to our KEGG pathway analysis, miR-99a-5p significantly
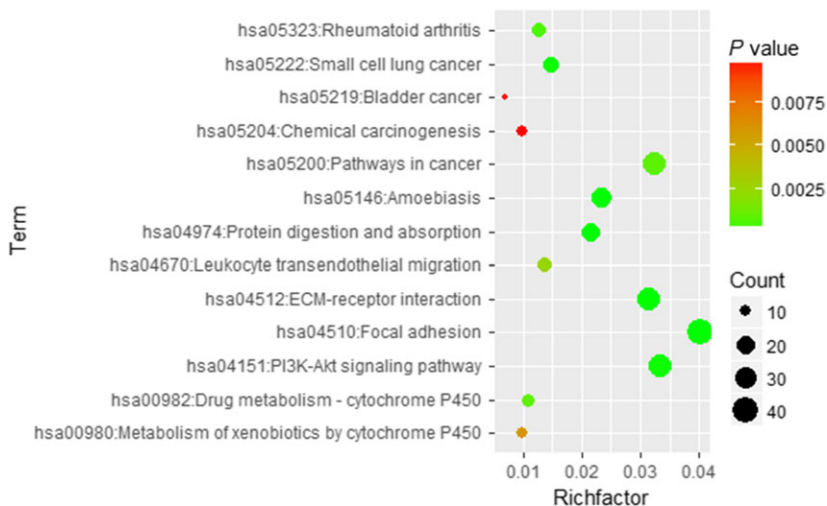
Fig. 12. Bubble diagram of KEGG pathway for HNSCC. Significant pathways with *P* value < 0.01 were plotted by R language.
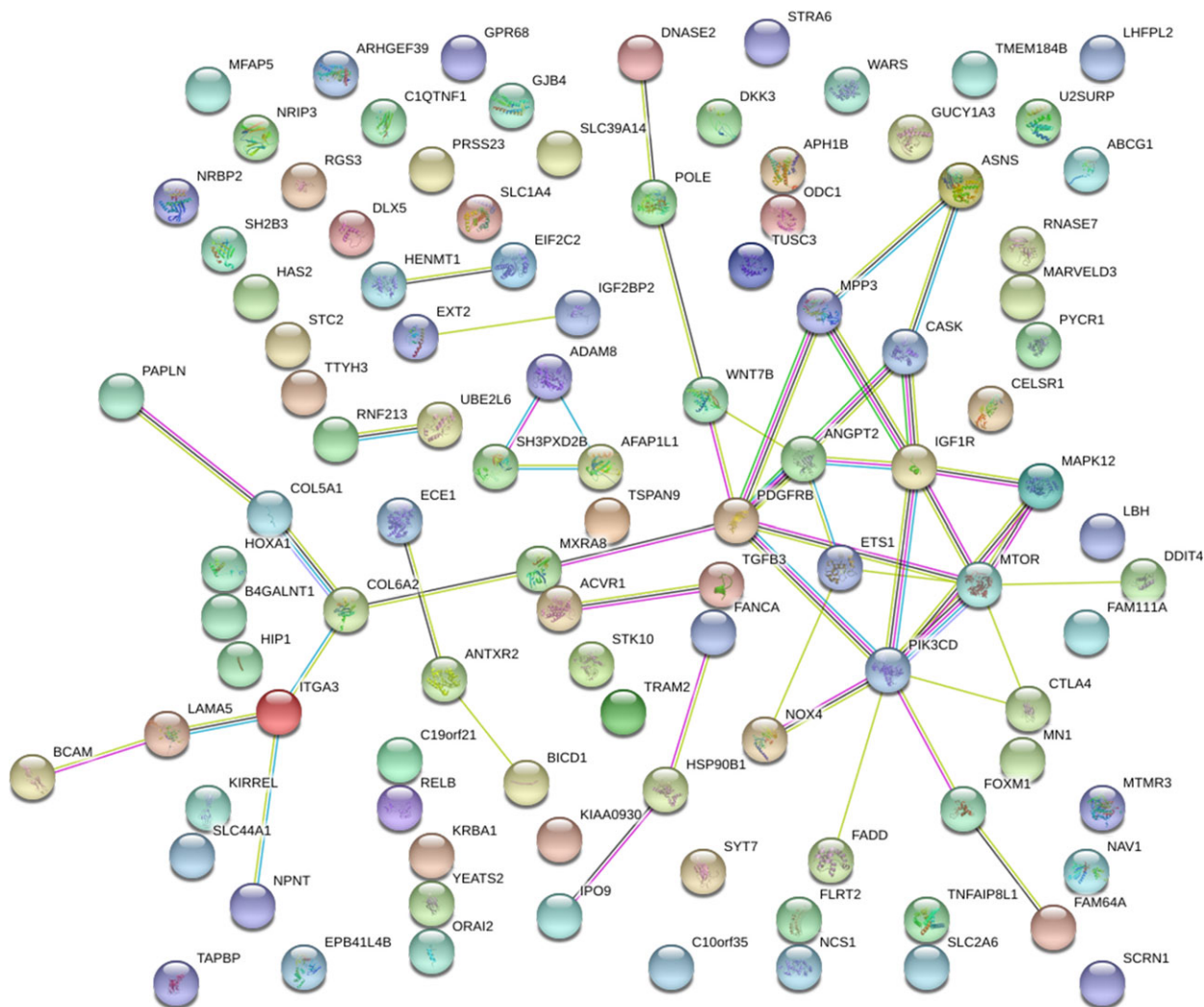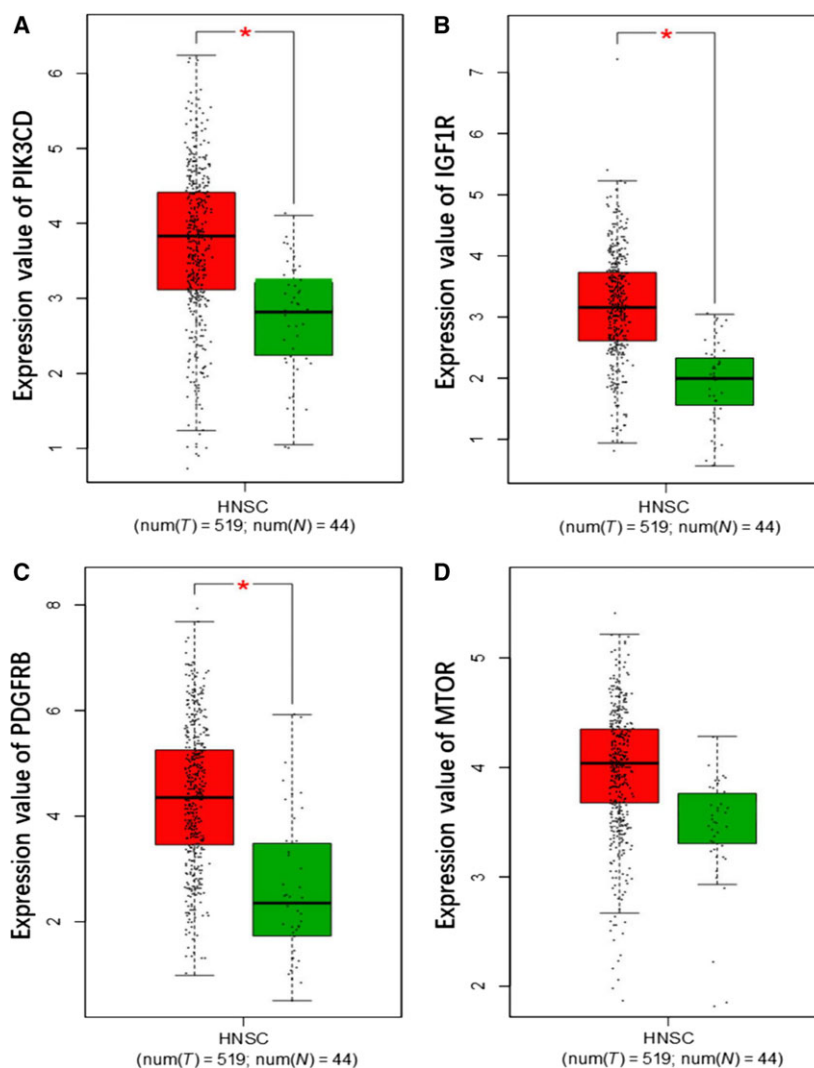

Fig. 13. PPI network of 103 promising target genes of miR-99a-5p in HNSCC.

Fig. 14. Expression analysis of four hub genes in 44 normal tissues and 519 HNSCC tissues based on GEPIA. (A) Expression value of *PIK3CD*. (B) Expression value of *IGF1R*. (C) Expression value of *PDGFRB*. (D) Expression value of *MTOR*.

affected the progression of HNSCC by regulating the PI3K-Akt signaling pathway, of which the predicted target genes, phosphatidylinositol-4,5-bisphosphate 3-kinase catalytic subunit data (*PIK3CD*), insulin-like growth factor 1 receptor (*IGFR1*), platelet-derived growth factor receptor, beta polypeptide (*PDGFRB*), and mechanistic target of rapamycin (*MTOR*) were involved.

The PI3K-Akt signaling pathway, concretely explained as the phosphatidylinositol 3-kinase (PI3K)/AKT/mammalian target of the rapamycin (mTOR) signaling pathway, is aberrant in many types of cancer [60–63]. The involved *PIK3CD*, *IGFR1*, *PDGFRB*, and *MTOR4*, also screened out by PPI construction, were further utilized to analyze the correlations with miR-99a-5p. We found that the four hub genes all exhibited higher expression levels in HNSCC tissues than in normal tissues, gaining more possibility to be the target genes of miR-99a-5p. Interestingly, a negative correlation was found between these four genes and miR-99a-5p, with *PIK3D* and *IGFR1* showing significant negative correlation with miR-99a-5p in HNSCC and *PDGFRB* and *MTOR* showing a mild negative correlation. Thus, together with the findings of previous researches and our results, we speculated that the dysfunctional PI3K-Akt signaling pathway was implicated in the development of HNSCC. Moreover, it seems that PI3K-Akt signaling pathway was regulated by miR-99a-5p according to the statistical correlation analysis, which further provided evidence for the
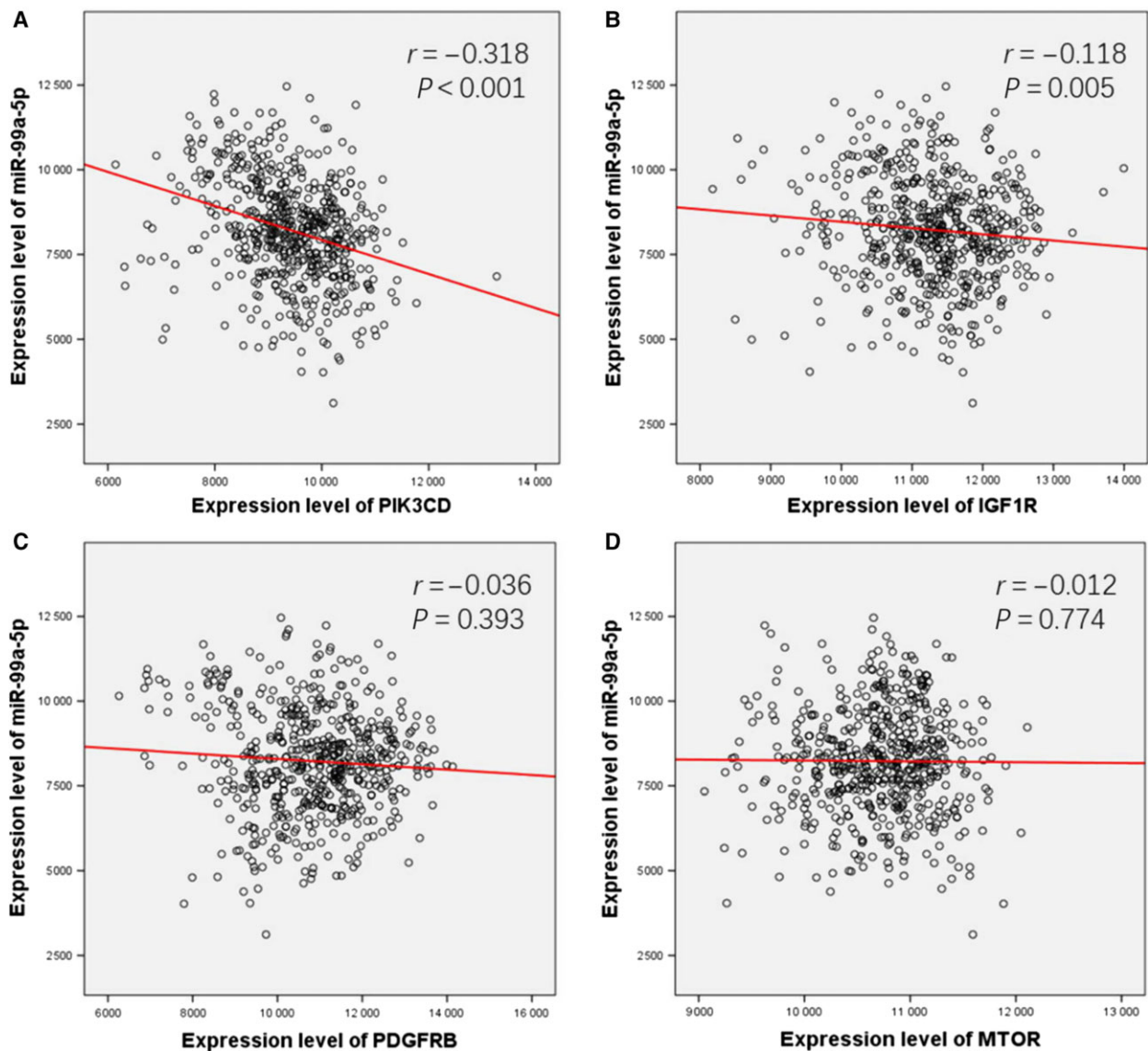
Fig. 15. Spearman's correlation analysis. Expression value of *PIK3CD* (A), *IGF1R* (B), *PDGFRB* (C), and *MTOR* (D) and their correlations with miR-99a-5p.

potential clinical value of miR-99a-5p detection in HNSCC.

Statistical analysis of miR-99a-5p expression would confirm our speculation. Previous studies have suggested that repressed miR-99a-5p may contribute to tumorigenesis via being unable to control the target genes. Thus far, no study has specifically analyzed the miR-99a-5p expression level in HNSCC, but several studies have demonstrated the lower expression of miR-99a-5p in HNSCC [46,51,59]. According to our GEO meta-analysis and TCGA data mining results, the miR-99a-5p expression level was markedly lower in HNSCC than in normal tissues. In addition, miR-99a-

5p expression was higher in low neoplasm histological grades than high histological grades, and the patient's age may also be a possible clinical parameter. Furthermore, we found that miR-99a-5p showed significance in diagnostic and prognostic tests; however, due to limited body fluid samples, the results could not be used as representative and its diagnostic applicability in the clinical setting could not be determined. Thus, additional studies are needed to demonstrate the clinical role of miR-99a-5p in the diagnosis and prognosis of HNSCC.

This study has some limitations. First, the different miRNA extraction methods may disturb the results

of our meta-analysis. Second, the HNSCC and corresponding samples were mostly derived from tissue sections, lead to an unverified diagnostic value. Third, although we utilized TCGA data to expand our data, the big gap between the quantity of cancerous and noncancerous tissues brought down the reliability. And fourth, the resource of online protein databases and relevant immunohistochemical staining samples were limited so that we could not further validate the function of miR-99a-5p via the protein level of hub genes. Despite these limitations, based on our meta-analysis, the results suggest that miR-99a-5p expression was significantly lower in HNSCC than in normal tissue. Biological analysis also suggested that miR-99a-5p may participate in HNSCC by suppressing the hub genes, *PIK3CD*, *IGFR1*, *PNGFRB*, and *MTOR*.

In general, our study confirmed that miR-99a-5p might be a tumor suppressor in HNSCC with downregulated expression in HNSCC tissues, via the PI3K-Akt signaling pathway. Further studies are required to elucidate the role of miR-99a-5p in diagnosis and prognosis for HNSCC and provide the basis for that miR-99a-5p execute its function via the protein level of the targets, especially those hub genes predicted by our research.

Acknowledgements

Author contributions

YQ, KH, FW, and YF conceived and designed the study. YC and JY collected, extracted, and analyzed the data. YQ and KH guided the statistical process and ensured the necessary graphs. YC and JY wrote the manuscript. All authors read and approved the final manuscript.

References

1 Liu S, Ye D, Wang T, Guo W, Song H, Liao Y, Xu D, Zhu H, Zhang Z and Deng J (2017) Repression of GPRC5A is associated with activated STAT3, which contributes to tumor progression of head and neck squamous cell carcinoma. *Cancer Cell Int* 17, 34.

2 Au JK, Alonso J, Kuan EC, Arshi A and St John MA (2017) Primary squamous cell carcinoma of the thyroid: a population-based analysis. *Otolaryngol Head Neck Surg* 157, 25–29.

3 Feng JF, Chen S and Yang X (2017) Combination of c-reactive protein and squamous cell carcinoma antigen in predicting postoperative prognosis for patients with squamous cell carcinoma of the esophagus. *Oncotarget* 8, 63132–63139.

4 Gu Z, Fang X, Li C, Chen C, Liang G, Zheng X and Fan Q (2017) Increased PTPRA expression leads to poor prognosis through c-Src activation and G1 phase progression in squamous cell lung cancer. *Int J Oncol* 51, 489–497.

5 Taneja Y, Ram P, Dhaked SK and Sen TK (2017) Squamous cell carcinoma penis in a case of urethral stricture due to lichen sclerosus balanitis xerotica obliterans: a case report and review of literature. *J Clin Diagn Res* 11, PD17–PD18.

6 Moriyama H, Kajiwara M and Yonehara S (2016) Primary squamous cell carcinoma of the prostate in which docetaxel therapy was effective : a case report. *Hinyokika Kiyo* 62, 259–264.

7 Terada T (2010) Synchronous squamous cell carcinoma of the kidney, squamous cell carcinoma of the ureter, and sarcomatoid carcinoma of the urinary bladder: a case report. *Pathol Res Pract* 206, 379–383.

8 Fedus T, Ras R, Ksiazek M, Filipowska J, Kaznowska E, Skret A, Skret-Magierlo J and Barnas E (2017) Primary vaginal squamous cell carcinoma with bladder involvement in uterine prolapsed patient: case report. *Medicine (Baltimore)* 96, e8993.

9 Ellingsen C, Andersen LM, Galappathi K and Rofstad EK (2015) Hypoxia biomarkers in squamous cell carcinoma of the uterine cervix. *BMC Cancer* 15, 805.

10 Sterba KR, Garrett-Mayer E, Carpenter MJ, Tooze JA, Hatcher JL, Sullivan C, Tetrick LA, Warren GW, Day TA, Alberg AJ *et al.* (2017) Smoking status and symptom burden in surgical head and neck cancer patients. *Laryngoscope* 127, 127–133.

11 Sawabe M, Ito H, Oze I, Hosono S, Kawakita D, Tanaka H, Hasegawa Y, Murakami S and Matsuo K (2017) Heterogeneous impact of alcohol consumption according to treatment method on survival in head and neck cancer: a prospective study. *Cancer Sci* 108, 91–100.

12 Udager AM and McHugh JB (2017) Human papillomavirus-associated neoplasms of the head and neck. *Surg Pathol Clin* 10, 35–55.

13 Schrock A, Leisse A, de Vos L, Gevensleben H, Droge F, Franzen A, Wachendorfer M, Schrock F, Ellinger J, Teschke M *et al.* (2017) Free-circulating methylated DNA in blood for diagnosis, staging, prognosis, and monitoring of head and neck squamous cell carcinoma patients: an observational prospective cohort study. *Clin Chem* 63, 1288–1296.

14 Cui L, Cheng S, Liu X, Messadi D, Yang Y and Hu S (2016) Syntenin-1 is a promoter and prognostic marker

of head and neck squamous cell carcinoma invasion and metastasis. *Oncotarget* **7**, 82634–82647.

15 Yu V, Singh P, Rahimy E, Zheng H, Kuo SZ, Kim E, Wang-Rodriguez J and Ongkeko WM (2016) RNA-seq analysis identifies key long non-coding RNAs connected to the pathogenesis of alcohol-associated head and neck squamous cell carcinoma. *Oncol Lett* **12**, 2846–2853.

16 Rothenberg SM and Ellisen LW (2012) The molecular pathogenesis of head and neck squamous cell carcinoma. *J Clin Invest* **122**, 1951–1957.

17 Xu CZ, Jiang C, Wu Q, Liu L, Yan X and Shi R (2016) A feed-forward regulatory loop between HuR and the long noncoding RNA HOTAIR promotes head and neck squamous cell carcinoma progression and metastasis. *Cell Physiol Biochem* **40**, 1039–1051.

18 Ma SR, Mao L, Deng WW, Li YC, Bu LL, Yu GT, Zhang WF and Sun ZJ (2017) AGR2 promotes the proliferation, migration and regulates epithelial-mesenchymal transition in salivary adenoid cystic carcinoma. *Am J Transl Res* **9**, 507–519.

19 Wang C, Cheng Y, Liu H, Xu Y, Peng H, Lang J, Liao J, Liu H, Liu H and Fan J (2016) Pectolinarigenin suppresses the tumor growth in nasopharyngeal carcinoma. *Cell Physiol Biochem* **39**, 1795–1803.

20 Huang J, Zhang J, Shi C, Liu L and Wei Y (2016) Survival, recurrence and toxicity of HNSCC in comparison of a radiotherapy combination with cisplatin versus cetuximab: a meta-analysis. *BMC Cancer* **16**, 689.

21 Mohanti BK, Thakar A, Kaur J, Bahadur S, Malik M, Gandhi AK, Bhasker S and Sharma A (2017) Postoperative radiotherapy dose requirement in standard combined-modality practice for head and neck squamous cell carcinoma: analysis of salient surgical and radiotherapy parameters in 2 cohorts. *Head Neck* **39**, 1788–1796.

22 Sun W, Wei FQ, Li WJ, Wei JW, Zhong H, Wen YH, Lei WB, Chen L, Li H, Lin HQ et al. (2017) A positive-feedback loop between tumour infiltrating activated Treg cells and type 2-skewed macrophages is essential for progression of laryngeal squamous cell carcinoma. *Br J Cancer* **117**, 1631–1643.

23 Hilly O, Strenov Y, Rath-Wolfson L, Hod R, Shkedy Y, Mizrachi A, Koren R and Shpitzer T (2016) The predictive value of dendritic cells in early squamous cell carcinoma of the tongue. *Pathol Res Pract* **212**, 1138–1143.

24 Kumamoto T, Seki N, Mataki H, Mizuno K, Kamikawaji K, Samukawa T, Koshizuka K, Goto Y and Inoue H (2016) Regulation of TPD52 by antitumor microRNA-218 suppresses cancer cell migration and invasion in lung squamous cell carcinoma. *Int J Oncol* **49**, 1870–1880.

25 Mizuno K, Seki N, Mataki H, Matsushita R, Kamikawaji K, Kumamoto T, Takagi K, Goto Y, Nishikawa R, Kato M et al. (2016) Tumor-suppressive microRNA-29 family inhibits cancer cell migration and invasion directly targeting LOXL2 in lung squamous cell carcinoma. *Int J Oncol* **48**, 450–460.

26 Powrozek T, Kuznar-Kaminska B, Dziedzic M, Mlak R, Batura-Gabryel H, Sagan D, Krawczyk P, Milanowski J and Malecka-Massalska T (2017) The diagnostic role of plasma circulating precursors of miRNA-944 and miRNA-3662 for non-small cell lung cancer detection. *Pathol Res Pract* **213**, 1384–1387.

27 Nunez Lopez YO, Victoria B, Golusinski P, Golusinski W and Masternak MM (2018) Characteristic miRNA expression signature and random forest survival analysis identify potential cancer-driving miRNAs in a broad range of head and neck squamous cell carcinoma subtypes. *Rep Pract Oncol Radiother* **23**, 6–20.

28 Suetsugu T, Koshizuka K, Seki N, Mizuno K, Okato A, Arai T, Misono S, Uchida A, Kumamoto T and Inoue H (2018) Downregulation of matrix metalloproteinase 14 by the antitumor miRNA, miR-150-5p, inhibits the aggressiveness of lung squamous cell carcinoma cells. *Int J Oncol* **52**, 913–924.

29 Wang HB, Jiang ZB and Li M (2014) Research on the typical miRNA and target genes in squamous cell carcinoma and adenocarcinoma of esophagus cancer with DNA microarray. *Pathol Oncol Res* **20**, 245–252.

30 Zhang X, Gee H, Rose B, Lee CS, Clark J, Elliott M, Gamble JR, Cairns MJ, Harris A, Khoury S et al. (2016) Regulation of the tumour suppressor PDCD4 by miR-499 and miR-21 in oropharyngeal cancers. *BMC Cancer* **16**, 86.

31 Irani S (2016) miRNAs signature in head and neck squamous cell carcinoma metastasis: a literature review. *J Dent (Shiraz)* **17**, 71–83.

32 Sun X, Xiao D, Xu T and Yuan Y (2016) miRNA-24-3p promotes cell proliferation and regulates chemosensitivity in head and neck squamous cell carcinoma by targeting CHD5. *Future Oncol* **12**, 2701–2712.

33 Moratin J, Hartmann S, Brands R, Brisam M, Mutzbauer G, Scholz C, Seher A, Muller-Richter U, Kubler AC and Linz C (2016) Evaluation of miRNA-expression and clinical tumour parameters in oral squamous cell carcinoma (OSCC). *J Craniomaxillofac Surg* **44**, 876–881.

34 Li J, Song ZJ, Wang YY, Yin Y, Liu Y and Nan X (2016) Low levels of serum miR-99a is a predictor of poor prognosis in breast cancer. *Genet Mol Res* **15**, 1–8.

35 Li Y, Zhang Z, Zhang X, Lin Y, Luo T, Xiao Z and Zhou Q (2016) A dual PI3K/AKT/mTOR signaling inhibitor miR-99a suppresses endometrial carcinoma. *Am J Transl Res* **8**, 719–731.

36 Xing B and Ren C (2016) Tumor-suppressive miR-99a inhibits cell proliferation via targeting of TNFAIP8 in osteosarcoma cells. *Am J Transl Res* **8**, 1082–1090.

37 Feng Y, Kang Y, He Y, Liu J, Liang B, Yang P and Yu Z (2014) microRNA-99a acts as a tumor suppressor and is down-regulated in bladder cancer. *BMC Urol* **14**, 50.

38 Gu W, Fang S, Gao L, Tan Y and Yang Z (2013) Clinic significance of microRNA-99a expression in human lung adenocarcinoma. *J Surg Oncol* **108**, 248–255.

39 Li D, Liu X, Lin L, Hou J, Li N, Wang C, Wang P, Zhang Q, Zhang P, Zhou W et al. (2011) MicroRNA-99a inhibits hepatocellular carcinoma growth and correlates with prognosis of patients with hepatocellular carcinoma. *J Biol Chem* **286**, 36677–36685.

40 Cappuzzo F, Sacconi A, Landi L, Ludovini V, Biagioni F, D'Incecco A, Capodanno A, Salvini J, Corgna E, Cupini S et al. (2014) MicroRNA signature in metastatic colorectal cancer patients treated with anti-EGFR monoclonal antibodies. *Clin Colorectal Cancer* **13**, 37–45. e4.

41 Oliveira RC, Ivanovic RF, Leite KRM, Viana NI, Pimenta RCA, Junior JP, Guimaraes VR, Morais DR, Abe DK, Nesrallah AJ et al. (2017) Expression of micro-RNAs and genes related to angiogenesis in ccRCC and associations with tumor characteristics. *BMC Urol* **17**, 113.

42 Wang X, Li Y, Qi W, Zhang N, Sun M, Huo Q, Cai C, Lv S and Yang Q (2015) MicroRNA-99a inhibits tumor aggressive phenotypes through regulating HOXA1 in breast cancer cells. *Oncotarget* **6**, 32737–32747.

43 Yang Z, Han Y, Cheng K, Zhang G and Wang X (2014) miR-99a directly targets the mTOR signalling pathway in breast cancer side population cells. *Cell Prolif* **47**, 587–595.

44 Yu SH, Zhang CL, Dong FS and Zhang YM (2015) miR-99a suppresses the metastasis of human non-small cell lung cancer cells by targeting AKT1 signaling pathway. *J Cell Biochem* **116**, 268–276.

45 Zhang Y, Xu W, Ni P, Li A, Zhou J and Xu S (2016) MiR-99a and MiR-491 regulate cisplatin resistance in human gastric cancer cells by targeting CAPNS1. *Int J Biol Sci* **12**, 1437–1447.

46 Chen D, Cabay RJ, Jin Y, Wang A, Lu Y, Shah-Khan M and Zhou X (2013) MicroRNA deregulations in head and neck squamous cell carcinomas. *J Oral Maxillofac Res* **4**, e2.

47 Hou B, Ishinaga H, Midorikawa K, Shah SA, Nakamura S, Hiraku Y, Oikawa S, Murata M and Takeuchi K (2015) Circulating microRNAs as novel prognosis biomarkers for head and neck squamous cell carcinoma. *Cancer Biol Ther* **16**, 1042–1046.

48 Tang Z, Li C, Kang B, Gao G, Li C and Zhang Z (2017) GEPIA: a web server for cancer and normal gene expression profiling and interactive analyses. *Nucleic Acids Res* **45**, W98–W102.

49 Kuo YZ, Tai YH, Lo HI, Chen YL, Cheng HC, Fang WY, Lin SH, Yang CL, Tsai ST and Wu LW (2014) MiR-99a exerts anti-metastasis through inhibiting myotubularin-related protein 3 expression in oral cancer. *Oral Dis* **20**, e65–e75.

50 Yen YC, Shiah SG, Chu HC, Hsu YM, Hsiao JR, Chang JY, Hung WC, Liao CT, Cheng AJ, Lu YC et al. (2014) Reciprocal regulation of microRNA-99a and insulin-like growth factor I receptor signaling in oral squamous cell carcinoma cells. *Mol Cancer* **13**, 6.

51 Chen Z, Jin Y, Yu D, Wang A, Mahjabeen I, Wang C, Liu X and Zhou X (2012) Down-regulation of the microRNA-99 family members in head and neck squamous cell carcinoma. *Oral Oncol* **48**, 686–691.

52 Shi Y, Bo Z, Pang G, Qu X, Bao W, Yang L and Ma Y (2017) MiR-99a-5p regulates proliferation, migration and invasion abilities of human oral carcinoma cells by targeting NOX4. *Neoplasma* **64**, 666–673.

53 Wang JG, Tang WP, Liao MC, Liu YP and Ai XH (2017) MiR-99a suppresses cell invasion and metastasis in nasopharyngeal carcinoma through targeting HOXA1. *Onco Targets Ther* **10**, 753–761.

54 Gambari R, Brognara E, Spandidos DA and Fabbri E (2016) Targeting oncomiRNAs and mimicking tumor suppressor miRNAs: new trends in the development of miRNA therapeutic strategies in oncology (Review). *Int J Oncol* **49**, 5–32.

55 Nguyen DD and Chang S (2017) Development of novel therapeutic agents by inhibition of oncogenic MicroRNAs. *Int J Mol Sci* **19**, E65.

56 Mei LL, Qiu YT, Huang MB, Wang WJ, Bai J and Shi ZZ (2017) MiR-99a suppresses proliferation, migration and invasion of esophageal squamous cell carcinoma cells through inhibiting the IGF1R signaling pathway. *Cancer Biomark* **20**, 527–537.

57 Sun M, Hong S, Li W, Wang P, You J, Zhang X, Tang F, Wang P and Zhang C (2016) MiR-99a regulates ROS-mediated invasion and migration of lung adenocarcinoma cells by targeting NOX4. *Oncol Rep* **35**, 2755–2766.

58 Doghman M, El Wakil A, Cardinaud B, Thomas E, Wang J, Zhao W, Peralta-Del Valle MH, Figueiredo BC, Zambetti GP and Lalli E (2010) Regulation of insulin-like growth factor-mammalian target of rapamycin signaling by microRNA in childhood adrenocortical tumors. *Cancer Res* **70**, 4666–4675.

59 Yan B, Fu Q, Lai L, Tao X, Fei Y, Shen J, Chen Z and Wang Q (2012) Downregulation of microRNA 99a in oral squamous cell carcinomas contributes to the growth and survival of oral cancer cells. *Mol Med Rep* **6**, 675–681.

60 Ersahin T, Tuncbag N and Cetin-Atalay R (2015) The PI3K/AKT/mTOR interactive pathway. *Mol BioSyst* **11**, 1946–1954.

61 Kumar D, Haldar S, Gorain M, Kumar S, Mulani FA, Yadav AS, Miele L, Thulasiram HV and Kundu GC (2018) Epoxyazadiradione suppresses breast tumor growth through mitochondrial depolarization and caspase-dependent apoptosis by targeting PI3K/Akt pathway. *BMC Cancer* **18**, 52.

62 Shi L, Zhao SM, Luo Y, Zhang AW, Wei LH, Xie ZY, Li YY and Ma W (2017) MiR-375: a prospective regulator in medullary thyroid cancer based on microarray data and bioinformatics analyses. *Pathol Res Pract* **213**, 1344–1354.

63 Ye J, Huang J, Xu J, Huang Q, Wang J, Zhong W, Lin X, Li Y and Lin X (2017) ERp29 controls invasion and metastasis of gastric carcinoma by inhibition of epithelial-mesenchymal transition via PI3K/Akt signaling pathway. *BMC Cancer* **17**, 626.

Supporting information

Additional Supporting Information may be found online in the supporting information section at the end of the article:

Fig. S1. (A-K): Scatter plots of miR-99a-5p expression data in normal and HNSCC tissues in the other 11 microarrays without statistical significance. (L-X): ROC curves of the other 13 microarrays without statistical significance.